Pergamon

Scripta Materialia, Vol. 39, Nos. 4/5, pp. 545–554, 1998
Elsevier Science Ltd

1359-6462/98 $19.00 + .00

PII S1359-6462(98)00195-X

YIELDING AND STRAIN HARDENING OF THIN METAL FILMS ON SUBSTRATES

William D. Nix
Department of Materials Science and Engineering, Stanford University, Stanford CA 94305-2205

(Received in final form May 15, 1998)

Introduction

It is now well-known that thin film materials are much stronger than their bulk counterparts. The high strengths can be caused, in part, by the fine grain sizes commonly found in thin films. However, single crystal thin films are also much stronger than bulk materials [1]. Venkatraman and Bravman [2], for example, have shown that both film thickness and grain size make important contributions to flow strength of Al films on Si substrates. They showed that the film strength varies inversely with the film thickness, both for very coarse grained samples, in which the grain size makes no contribution to the strength, and for fine grained samples. In the present paper we focus our attention on the dislocation processes responsible for these film thickness strengthening effects.

Figure 1 shows the type of experiment commonly used to study plastic deformation and strain hardening in thin metal films. The figure shows how the biaxial stresses in Al and Cu films on Si substrates change during thermal cycling. Because of differences in thermal expansion, the metal films are forced to deform in biaxial compression and tension, respectively, as the bilayer structures are heated and cooled. The tension stresses at room temperature reach several hundred MPa, much higher stresses than could be sustained by these pure metals in bulk. Even at very high temperatures, the compressive stresses are about 100 MPa, at least an order of magnitude higher than the flow stresses for bulk pure metals. The figure also shows the very high strain hardening rates exhibited by thin metal films on substrates. On cooling from the highest temperatures, the films first deform elastically and then, at about 300°C, begin to yield in tension at about 100 MPa. On cooling to room temperature the flow stress increases very significantly, up to 200–300 MPa, in spite of the very small plastic strains involved. This amounts to a very high rate of strain hardening, very much higher than the Stage II rate of work hardening for these metals, for example. Our treatment of the strength of thin metal films on substrates will include a discussion of these high rates of strain hardening.

To understand dislocation strengthening in thin films on substrates it is instructive to consider how a single dislocation might move on its slip plane within the film. Figure 2 shows the motion of a dislocation in a single crystal film subjected to a simple in-plane biaxial loading. Because the dislocation is confined to move in the film and not in the substrate, a “misfit” dislocation will be deposited near the film/substrate interface as the dislocation glides on its slip plane. This situation is like the process of strain relaxation in heteroepitaxial thin films, except that the metal film considered here need not be epitaxial with the substrate. Matthews et al. [3] were the first to show that a critical stress is needed to create misfit dislocations by the process shown in Fig. 2. Freund [4–5] later analyzed the stability of such dislocation structures and derived a rigorous relationship for the critical stress needed to cause dislocation motion in thin films. For the coordinate system shown in Fig. 2, and using the

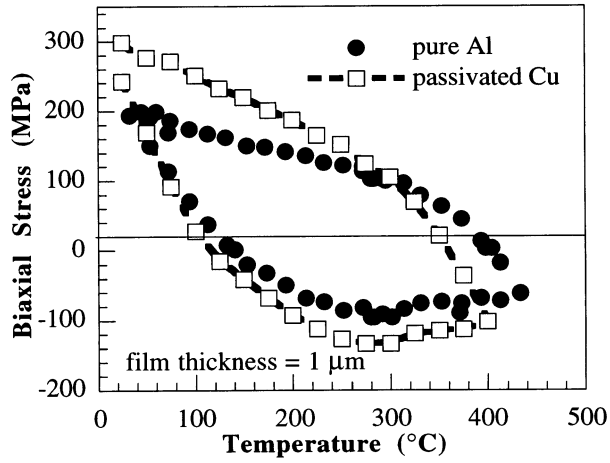

Figure 1. Stress-temperature plots for Al and Cu thin films on a Si substrate. High strengths and high strain hardening rates are indicated. (Data provided by R.P. Vinci, Stanford University.)

RH/SF convention for the Burgers vector and the sense vector shown, the critical stress for dislocation motion in the film was shown by Freund [5] to be

$$\sigma = -\frac{\mu}{4\pi h b_1(1-\nu)}\left\{[b_1^2 + b_2^2 + (1-\nu)b_3^2]Log\left(\frac{2h}{b}\right) - \tfrac{1}{2}(b_1^2 + b_2^2)\right\}, \tag{1}$$

where b_i are the components of the Burgers vector (b_1 is negative for the dislocation shown in Fig. 2), μ and ν are the elastic shear modulus and Poisson's ratio, respectively, of both film and substrate and h is the film thickness. A dislocation core cut-off radius of b is taken in this relation. A relation similar to this was given by Embury and Hirth [6], based on earlier work of Ashby [7].

For the case of an unpassivated (111) oriented film (typical for FCC metal films) with slip on the $<011>\{111\}$ slip system, Freund's formula can be used to determine the critical biaxial stress needed to move the dislocation against the drag force associated with the misfit dislocation. Using $b_1 = -b/2\sqrt{3}$, $b_2 = b\sqrt{2}/\sqrt{3}$ and $b_3 = -b/2$, the result is

$$\sigma_c = \frac{\sqrt{3}\mu b}{8\pi(1-\nu)h}\left[(4-\nu)Log\left(\frac{2h}{b}\right) - \frac{3}{2}\right]. \tag{2}$$

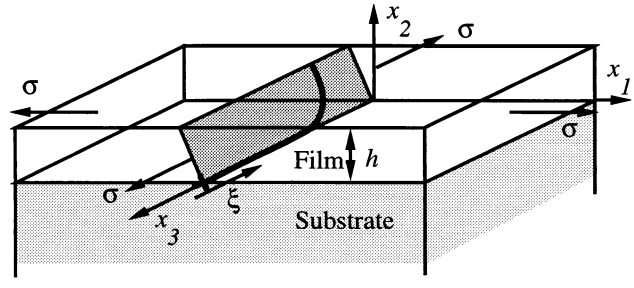

Figure 2. Motion of a threading dislocation segment in a thin film leaving a misfit dislocation in its wake.

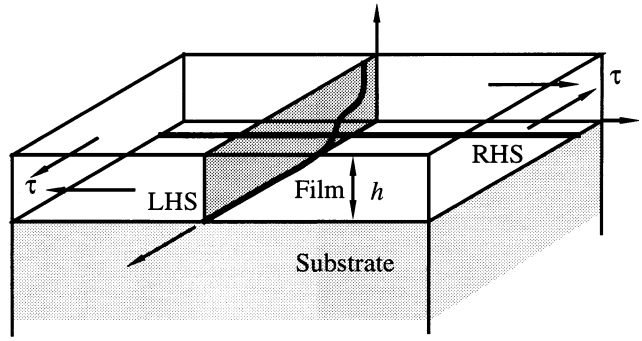

Figure 3. Screw dislocation model for dislocation motion and interaction in thin films on substrates.

We see immediately that the film strength depends strongly on the film thickness, varying approximately inversely with the film thickness, h^{-1}. Indeed, this dependence on film thickness is in close agreement with the experiments of Venkatraman and Bravman [2]. This equation predicts a biaxial strength of 23 MPa for a 1 μm thick Al film. As discussed below, this prediction increases by about a factor of two when the effect of the Al_2O_3 scale on the surface of Al is taken into account, because a dislocation dipole is created in the film as the dislocation moves and because the dislocations are repelled from the substrate and the Al_2O_3 scale. The higher strengths shown in Fig. 1 are caused both by dislocation interactions and grain size effects. In the present paper we study the effects of passivation and dislocation interactions on the strength of metal films on substrates. We also consider the effects of elastic rigidity of the substrate and passivation on the strength. As discussed below, we make use of a very simple dislocation model to study these effects.

Screw Dislocation Model

Here we consider a very simple model for plasticity of thin films, wherein the threading dislocation segment is imagined to be a pure edge dislocation on a slip plane perpendicular to the plane of the film and the misfit dislocation deposited in its wake is a pure screw. This is shown in Fig. 3 where the threading segment is beginning to interact with an orthogonal screw dislocation already present at the film/substrate interface. We note immediately that the vertical plane is not an actual slip plane and these dislocations would not respond to biaxial stresses present in real films. Instead, a shear stress, as shown in the figure, is assumed to be present. We use this model in an effort to simplify the interactions and to study the effects of substrate and passivation rigidity on the strengthening processes. This simple geometry is convenient because it permits an analysis of the elastic fields of the obstacles in terms of image dislocations [8–9]. The model captures the essential features of dislocation motion in a thin film on a substrate. We first evaluate the effects of the substrate and passivation moduli on the film strength. Then we use the model to estimate the strengthening effects of single and multiple dislocation obstacles. These results permit us to estimate the rate of strain hardening expected for thin metal films on substrates.

First consider the case of a bare thin film on a substrate having the same shear modulus as the film. Figure 4 depicts the process of dislocation motion and misfit formation at the film/substrate interface. For this process to occur spontaneously, the shear stress must be sufficiently large to supply the work

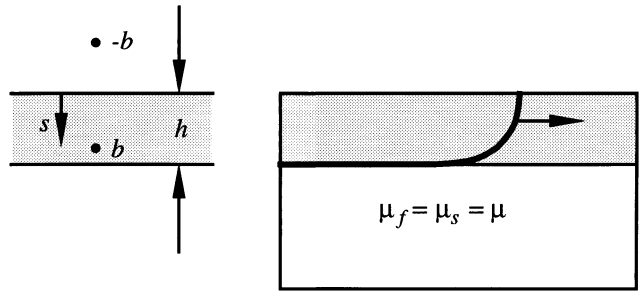

Figure 4. Dislocation motion in an unpassivated thin film on a substrate showing both the real dislocation and its image.

needed to form a unit length of misfit dislocation as the threading segment advances a unit distance. Equating the work available to the work required, we find

$$\tau_{channel} bh = W_{misfit} = \int_b^h f\, ds = \int_b^h \frac{\mu b^2}{4\pi s}\, ds = \frac{\mu b^2}{4\pi} Log\left(\frac{h}{b}\right), \tag{3}$$

which leads to the following expression for the film strength,

$$\tau_0 = \frac{\mu b}{4\pi h} Log\left(\frac{h}{b}\right). \tag{4}$$

Here the energy of the misfit dislocation is found using the method of images and is determined by calculating the work needed to move the real dislocation from very near the surface (a core radius, *b*, from the surface) to the film/substrate interface. This calculation involves the interaction force, *f*, between the real dislocation and its image, as shown in the figure. We call this a channeling process because the threading dislocation is forced to move in the narrow channel defined by the slip plane and the two surfaces of the film. The resulting expression for the film strength is similar in form to [2] and provides a useful reference for the strengthening effects to be described below. In all of the subsequent calculations described below we express the film strength as a multiple of τ_0.

Elastic Modulus Effects

Unpassivated Film—Single Misfit Dislocation

Consider a dislocation moving in a thin film with shear modulus μ_f on a more rigid substrate with shear modulus μ_s, as shown in Fig. 5. As the threading segment moves, the misfit dislocation will be deposited some distance away from the film/substrate interface, because of the elastic repulsion of the more rigid substrate. The most important images needed to describe the elastic field of the misfit dislocation are shown in the figure in their approximate positions; they are used to determine both the position of the misfit dislocation and its energy. A real dislocation of unit strength is shown in the film and the strengths of the images needed to satisfy the traction and displacement boundary conditions at the free surface and at the film/substrate interface are also shown. The image strength κ is defined as $\kappa = (\mu_s - \mu_f)/(\mu_s + \mu_f)$. Using the image fields, the stress needed to hold the misfit dislocation at a position *s* is found to be

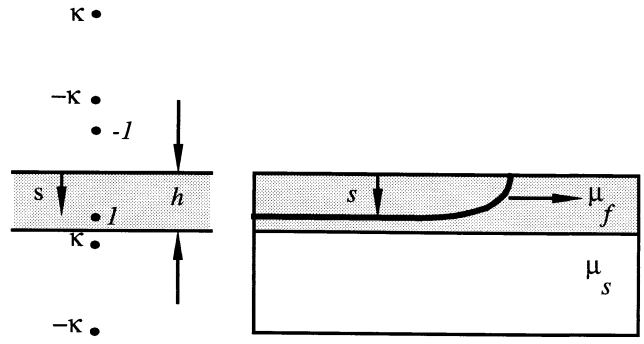

Figure 5. Motion of a dislocation in a thin film on a substrate with a higher shear modulus, showing the most important image dislocations.

$$\tau_{equil} = \frac{\mu_f b}{4\pi}\left[\frac{\kappa}{(h-s)} + \frac{1}{s} - \frac{\kappa}{(h+s)}\right], \tag{5}$$

and the corresponding shear stress needed to drive the threading dislocation in its channel at that same misfit position is

$$\tau_{channel} = \frac{\mu_f b}{4\pi s}\left[Log\left(\frac{s}{b}\right) + \kappa Log\left(\frac{h-b}{h-s}\right) - \kappa Log\left(\frac{h+s}{h+b}\right)\right]. \tag{6}$$

As the threading segment moves through the film, the equilibrium position of the misfit dislocation, s^{eq}, is set by the condition that these two stresses be the same, $\tau_{equil}(s^{eq}) = \tau_{channel}(s^{eq})$. Once the equilibrium position of the misfit is found, the corresponding stress can be found using either (5) or (6). A moderate effect of substrate modulus on the film strength is found by this analysis, the reference stress τ_0 being exceeded by only about 30% for very rigid substrates.

Passivated Film—Misfit Dislocation Dipole

We now consider the case of a thin metal film covered by a non-shearable passivation, such as silicon nitride, as shown in Fig. 6. In this case, dislocation motion in the film causes a misfit dislocation dipole to be deposited. One of the misfit dislocations is deposited near the film/substrate interface while the other is deposited near the film/passivation interface. Elastic interactions between the dislocations and

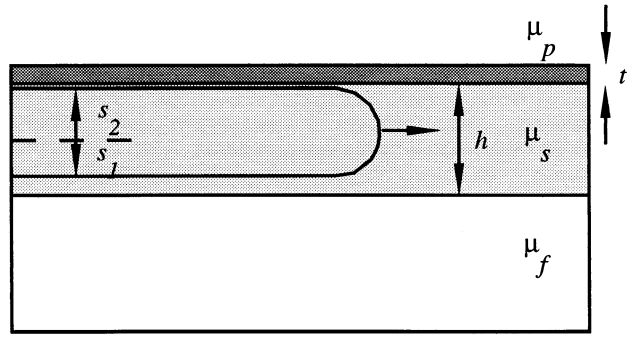

Figure 6. Dislocation dipole formation in a passivated film.

their images determines their equilibrium positions. Space does not permit the image solution for these misfit dislocations to be to be given here; it will be presented elsewhere. We simply state that two equilibrium positions, s_1^{eq} and s_2^{eq}, need to be determined to find the channeling stress. If $f_1(s_1,s_2)$ and $f_2(s_1,s_2)$ are the forces (per unit length) needed to hold the dislocations at positions s_1 and s_2 respectively, then the energy (per unit length) of the dipole is

$$W_{dipole} = \int_{s_1=b}^{s_1=s_1^{eq}} f_1(s_2 = 0)\, ds_1 + \int_{s_2=0}^{s_2=s_2^{eq}} f_2(s_1 = s_1^{eq})\, ds_2, \tag{7}$$

considering that the two dislocations start out at the center of the film a small distance, b, apart. The corresponding channeling stress is then

$$\tau_{channel} = \frac{W_{dipole}}{b(s_1^{eq} + s_2^{eq})}, \tag{8}$$

and the two interaction stresses are

$$\tau_1^{equil} = f_1(s_1^{eq}, s_2^{eq})/b \quad \text{and} \quad \tau_2^{equil} = f_2(s_1^{eq}, s_2^{eq})/b. \tag{9}$$

The equilibrium positions are found by solving

$$\tau_{channel}(s_1^{eq}, s_2^{eq}) = \tau_1^{equil}(s_1^{eq}, s_2^{eq}) = \tau_2^{equil}(s_1^{eq}, s_2^{eq}). \tag{10}$$

The strength of the film can then be found by computing the channeling stress. We find that when the substrate modulus is three times the film modulus (typical for Al on Si), the effect of a passivation of thickness $10b$ is to increase the film strength up to about 2.3 τ_o. For the case in which the elastic properties of both the substrate and passivation are about the same as the film, the strength of the film is 1.54 τ_0 for a passivation thickness of $10b$. Thus the elastic rigidity effects of the substrate and passivation amount to a strength enhancement of about 1.5 times the strength for the elastically homogeneous case.

An upper bound calculation of the effects of substrate and passivation rigidity can be made by considering that both the substrate and passivation are elastically rigid. A particularly simple image solution can be constructed for this case involving an infinite array of unit image dislocations of alternating sign. When this analysis is made an upper bound strength of is about 2.4 τ_0, almost independent of the film thickness is found. For comparison, the strength of a film bounded on both sides by semi-infinite substrates with the same shear modulus as the film is 2.0 τ_0.

Dislocation Interaction Effects

We consider now the effects of obstacle dislocations on the strength of thin metal films on substrates. Here the substrate and passivation, when present, are assumed to have the same elastic properties as the film. The strengthening effects to be described here are in addition to those that arise from elastic rigidity effects.

Unpassivated Film - Single Misfit Obstacle

A propagating dislocation may be repelled from a misfit dislocation already present at the film/substrate interface, provided the two dislocations have the right signs. In the present treatment we follow the

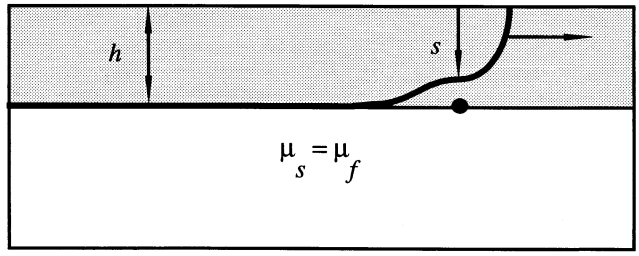

Figure 7. Dislocation interaction with a single misfit obstacle dislocation already present at the film/substrate interface.

approach of Freund [10] in estimating the blocking effect of such obstacle dislocations. The elastic field of the obstacle forces the moving dislocation to pass through the film at some distance away from the interface, as shown in Fig. 7. We will assume that the critical point in the passing process occurs just above the obstacle. At that point the stress needed to hold the misfit segment in equilibrium at a position s is given

$$\tau_{equil}(s) = \frac{\mu b}{4\pi}\left[\frac{2}{(h\text{-}s)} + \frac{2}{(h+s)} + \frac{1}{s}\right], \tag{11}$$

and the corresponding stress needed to drive the threading segment through the channel is

$$\tau_{channel}(s) = \frac{\mu b}{4\pi}\frac{1}{s}\int_b^s \left[\frac{4}{(h-s)} + \frac{4}{(h+s)} + \frac{1}{s}\right] ds. \tag{12}$$

We have used the method of images to describe the elastic fields of both the misfit segment and the obstacle dislocation in deriving these relations. We have assumed that the misfit segment is infinitely long and thus have ignored the contributions of the curved parts of the threading segment on the passing process. As before, the equilibrium passing position of the misfit segment, just above the obstacle, is set by the condition $\tau_{equil}(s^{eq}) = \tau_{channel}(s^{eq})$. Solving this equation for s^{eq} and using the result to find the strength of the film, we find a film strength of about 2.6 τ_0 for a 1 μm thin film. This strength enhancement depends only very weakly on the film thickness.

Passivated Film—Misfit Dipole Obstacle

For the case of a passivated film, a moving dislocation will interact with dislocation dipoles already present in the film. As shown in Fig. 8, for certain Burgers vectors, the moving dislocation will be

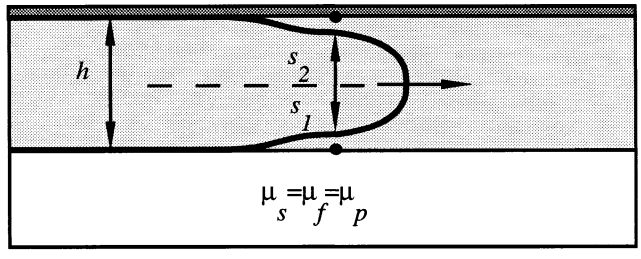

Figure 8. Dislocation interaction with a pre-existing misfit dislocation dipole obstacle.

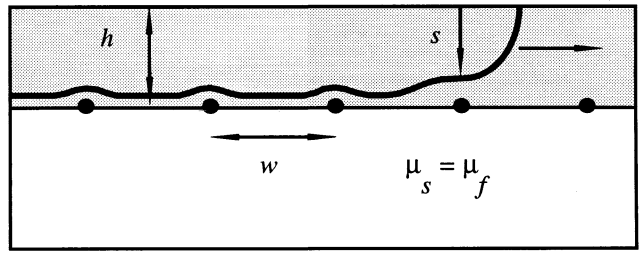

Figure 9. Dislocation interaction with an array of misfit obstacle dislocations in an unpassivated film.

forced to squeeze in between the two dislocations that comprise the misfit dipole obstacle. For this problem two equilibrium positions, s_1^{eq} and s_2^{eq}, need to be determined to find the channeling stress. Again using the image method to solve this problem, we find a film strength of about 4.4 τ_0 for a 1 μm film with a passivation thickness of 100 b. This enhancement depends only weakly on the thickness of the film and passivation.

This result, together with the effect of elastic rigidity discussed above, suggests that the strength of a passivated thin film might be enhanced by a factor of about $\approx 4.4 \times 1.5 = 6.6$ over the reference strength. For the 1 μm film discussed in the introduction, these combined strengthening effects would lead to a predicted film strength of about $\approx 6.6 \times 23\ MPa \approx 150 MPa$, a result which is in good agreement with experiment.

Multiple Obstacle Dislocations and Strain Hardening

As noted in the introduction, plastic deformation of thin metal films on substrates is characterized by very high rates of strain hardening. This hardening is caused by the storage of misfit dislocations near the film/substrate interface. To model this situation we consider the interaction of a moving dislocation with an array obstacle dislocation already present at the film/substrate interface, as shown in Fig. 9. For certain Burgers vectors, the misfit dislocation will be repelled from the obstacles, as shown, and this will increase the strength of the film in the manner already discussed. Again treating the misfit segment just above the obstacle as an infinitely long misfit dislocation and computing the elastic field of an infinite array of misfit dislocation obstacles using the method of images, we find

$$\tau_{equil}(s) = \frac{\mu b}{2w}\left[Coth\left(\left(\frac{h-s}{w}\right)\pi\right) + Coth\left(\left(\frac{h+s}{w}\right)\pi\right)\right] + \frac{\mu b}{4\pi s} \tag{13}$$

and

$$\tau_{channel}(s) = \frac{\mu b}{4\pi s}\int_b^s \left\{\frac{4\pi}{w}\left[Coth\left(\left(\frac{h-s}{w}\right)\pi\right) + Coth\left(\left(\frac{h+s}{w}\right)\pi\right)\right] + \frac{1}{s}\right\} ds, \tag{14}$$

where w is the spacing between uniformly spaced obstacle dislocations. These equations can be solved simultaneously to determine the strength of a film. Recognizing that the spacing between obstacle dislocations is directly related to the plastic strain in the film through $\gamma_{plastic} \approx b/w$, we may express the resulting strengths in terms of the total strain, $\gamma_{total} = \gamma_{elastic} + \gamma_{plastic} = (\tau/\mu) + (b/w)$, as shown graphically in Fig. 10. There we see that a very high rate of strain hardening is predicted for this situation, with the strain hardening rate being a significant fraction of the shear modulus. The estimate made here is probably an upper bound, as all of the obstacles considered repel the moving dislocation.

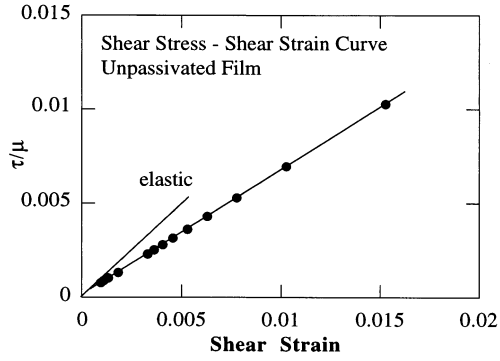

Figure 10. Predicted stress-strain curve using the model of Fig. 9 to describe the dislocation structure in the film.

In a real film, the obstacle dislocations would be of various signs and this would thus lessen the predicted strain hardening. Nevertheless, the very high strain hardening rates predicted are consistent with experiment. The stress-temperatures hysteresis curves shown in Fig. 11 for a thin single crystal film of Al on Si show extremely high rates of strain hardening on cooling. After the yield stress is exceeded, the biaxial stress in the film rises very steeply, as the film is deformed in biaxial tension on cooling. The association of this hardening with the storage of dislocations in the film is supported by both TEM and x-ray line broadening experiments [2].

Concluding Remarks

We have shown that the very high strengths and high strain hardening rates exhibited by thin metal films on substrates can be understood by considering the effects of confinement on the motion of dislocations. Both the substrate and passivation and the obstacle dislocations already present in the film narrow the channels through which dislocations can move and this leads to very significant strengthening and strain hardening.

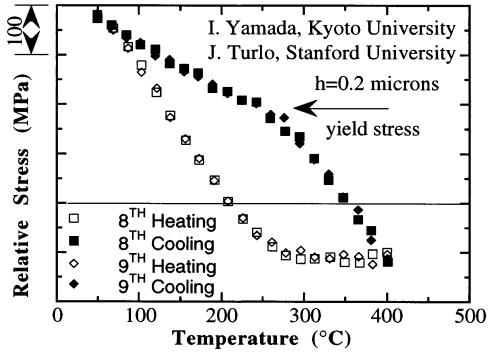

Figure 11. Stress-temperature hysteresis curves for a thin single crystal film of Al on Si, showing very high rates of strain hardening on cooling.

Acknowledgments

The support of this work by the Division of Materials Sciences, Office of Basic Energy Sciences of the United States Department of Energy under grant DE-FG03-89-ER45387 is gratefully acknowledged. The author also wishes to thank his friend and colleague, Professor D.M. Barnett, for assistance with some of the dislocation calculations.

References

1. W. D. Nix, Metall. Trans. 20A, 2217 (1989).
2. R. Venkatraman and J. C. Bravman, J. Materials Research, 7, 2040 (1992).
3. J. W. Matthews, S. Mader, and T. B. Light, J. Applied Physics, 41, 3800 (1970).
4. L. B. Freund, J. Appl. Phys., 54, 553 (1987).
5. L. B. Freund, Advances in Applied Mechanics. 30, 1, (1994).
6. J. D. Embury and J. P. Hirth, Acta Metall. et Mater. 42, 2051 (1994).
7. M. F. Ashby, Acta Metall., 14, 679 (1966).
8. A. K. Head, Phil. Mag., 44, 92 (1953).
9. M. L. Ovecoglu, M. F. Doerner, and W. D. Nix, Acta Metall., 35, 2947 (1987).
10. L. B. Freund, J. Appl. Phys., 68, 2073-2080 (1990).